A theoretical study of the structural, vibrational, and topological properties of charge distribution of the molecular complexes between furan and zeolites

L. Zeidabadinejad* and M. Dehestani

Department of Chemistry, Shahid Bahonar University of Kerman, Kerman, P.O. Box 76169, Iran.

Abstract. The main interaction between furan and zeolites leads to formation of a hydrogen bond between the O atom of furan and the OH groups of zeolites. The present work reports a theoretical study about the structural, vibrational, and topologic properties of charge distribution of the molecular complexes between furan and the series of acids sites of zeolites. The calculated structural parameters are the highest occupied molecular orbital energy (E_{HOMO}), the lowest unoccupied molecular orbital energy (E_{LUMO}), energy gap (ΔE), hardness (η), softness (S), absolute electronegativity (χ), electrophilicity index (ω), and the fractions of electrons transferred (ΔN) from zeolites molecules to furan. We show that the H atom of the bridged OH group of zeolite clusters attacks the O atom of furan.

1. Introduction

Furan is a five-membered heterocycle that plays a convenient role in the current organic chemistry and occurs in the structures of many natural products, pharmaceutical agrochemical compounds, and other commercial substances. Furans serve as initial substances for many important syntheses, form the structural units of various products, and represent the building blocks for the promising novel materials [1]. Hence, the physical chemistry, spectroscopy, and electronic structure of these molecules have attracted high attention. In particular, furan has been used as the electron acceptors in studies involving hydrogen bonding complexes [2,3].

Zeolites are crystalline aluminosilicate compounds which have been used as acid catalysts in many important industrial processes [4-6]. The acidic properties

of these materials arise from the presence of hydroxyl groups named acid sites of zeolites. These zeolites are very simple and small clusters of a huge crystal representing the acidic sites which were indicated as $H_3Si(OH)AlH_3$ (B_1), $(OH)_3Si(OH)Al(OH)_3$ (B_1OH), and $H_3Si(OH)Al(OH)_2OSiH_3$ (B_2). The optimized electronic structure, vibrational frequencies, topologic properties, and relationship between the Mulliken populations of the H atom of OH in these compounds have been reported at the HF and MP2/6-31G (d, p) theory levels [7,8].

The weak bases that have proton affinity in the 115-200 kcal mol^{-1} range can form hydrogen bonds with the structural Brønsted sites of acidic zeolites. The strength of hydrogen bond tends to increase as proton affinity of the base increases [9,10]. The interaction that occurs between bases with higher proton affinity and acidic zeolites is proton transfer and the creation of hydrogen bonded ionic pairs [10]. The spectroscopy data (UV-VIS and IR) shows that interaction of pyrrole, furan, and thiophene with zeolites leads to

---

*. Corresponding author. Tel.: +98 913 3458552
 E-mail addresses: lzeidabadi@yahoo.com (L. Zeidabadinejad); dehestani2002@yahoo.com (M. Dehestani)

the formation of hydrogen bond between the Brønsted acid sites and the π electron system of the heterocyclic molecules [9]. Then, at room temperature the hydrogen bonded complexes can change to protonated bases. The kind of hetroatom in the hetrocycle can influence the rate of this change so that the rate increases in the following order: pyrrole < thiophene < furan. In the presence of extra bases, analysis of the electronic spectra shows that the reaction between protonated species monomers gives entrapped oligomers with up to six conjugated double bonds [11].

Quantum Theory of Atoms In Molecule (QTAIM) analysis can be used to connect the changes in charge of the atoms in molecules. Since the QTAIM approach provides a great deal of information about the nature of bonding, we have explored the topological properties of electron density $\rho(r)$ and the Laplacian of the electron density $\nabla^2\rho(r)$ at various Bond Critical Points (BCPs) to characterize the presence of possible open-shell and closed-shell interactions in the coordination sphere. The QTAIM has been employed to elucidate the interaction between the O atom of furan and the H atoms of the bridged OH groups of the zeolite clusters giving a series of furan-zeolite molecular complexes. We have also applied charge analysis to investigate properties of the bond and electron charge transfer of the zeolite-furan complexes. We report a theoretical study about topologic properties of the charge distribution of these molecular complexes.

These results show that the furan zeolites molecular complexes are energetic and structurally stable. These results are analyzed in terms of the vibrational features of OH groups, the structural properties of complexes, and the energetic properties.

2. Computational procedure

All calculations were performed using Gaussian 03 package. For the isolated species and complexes, we have used Moller-Plesset second order perturbation theory MP2 method by employing cc-PVTZ basis set by Hehre et al., Parr and Yang [12,13] to study the geometric, electronic, and vibrational properties. Then corresponding frequency calculations were carried out at the same level to ensure that the optimized structures are true minima. The topologic properties of furan-zeolite complexes have been calculated using the theory of Bader of Atoms In Molecules (AIM) [14] as developed by Cioslowski and coworkers [15] in the Gaussian 03 set of programs [16].

The theory of AIM gives a particular quantum mechanical description for charge distribution, so that the analysis of molecular electron density distribution provides valuable information about many different chemical systems. Application of AIM theory to understand nature of the bonds in deeper detail is an interesting approach. Theory of AIM is based on the Critical Point (CP) of the molecular electronic charge density $\rho(r)$. These are points where the electronic density gradient $\nabla^2\rho(r)$ vanishes. The sign of $\nabla^2\rho(r)$ indicates whether the charge density is locally depleted ($\nabla^2\rho(r) > 0$) or locally concentrated ($\nabla^2\rho(r) < 0$). Thus, when negative curvatures dominate at the Bond Critical Point (BCP), electronic charge is locally concentrated within the region between atoms leading to an interaction named as covalent or polarized bonds and being characterized by large $\rho(r)$ values, $\nabla^2\rho(r) < 0$. For low $\rho(r)$ values, $\nabla^2\rho(r) > 0$, the interaction is now referred to as a closed-shell and is characterized by highly ionic bonds, hydrogen bonds, and Vander Waals interactions [15].

In the present study, we have applied the theory of Bader to characterize the topologic properties of electronic charge density of the interaction between furan and acid sites of zeolites. Molecular geometries and vibrational properties of furan, B_1, B_1OH, B_2 clusters, and the corresponding furan-zeolite complexes were calculated at the MP2/cc-PVTZ level theory.

3. Results and discussion

3.1. Geometric structure of complexes

The main goal of this work is to characterize the electronic and structural nature of the furan-zeolite interaction. We are concerned with geometric, vibrational, and electronic features of furan and its complexes.

Furan is a planar molecule and belongs to the C_{2v} symmetry group. Results for the C_{2v} optimized structure of furan with MP2/cc-PVTZ and B3LYP/cc-PVTZ levels of theory were reported previously by Mellouki et al., Szafran and Koput [17,18].

We start the calculations with clusters B_1, B_1OH, and B_2 whose structural, electronic, and conformational properties have been reported by Soscún et al. [8]. The B1OH structure is similar to the B_1 cluster, except OH groups substitute the terminal H atoms of Si and Al ones. The B_2 structure is a well-known cluster [7,8]. Figure 1 shows the structures of zeolites clusters. The optimized geometric parameters of isolated zeolite clusters (B_1, B_1OH, and B_2) are reported in Table 1. The MP2 results for the main bonds of these clusters are around the values of 1.683 Å for the Si–O bond, 1.828 Å for the Al–O bond, and 0.956 Å for the O–H bond.

In this work, we have considered a perpendicular interaction of the furan molecules with the bridged OH groups of zeolite clusters. When each B_1, B_1OH, or B_2 cluster approaches a furan molecule, a bond from the O atom of furan and the OH group of each cluster is formed giving the B_1−furan, B_1OH−furan, and B_2−furan stable complexes (Figure 2). The cor-

Table 1. Selected ground-state geometry parameters of B_1, B_1OH, and B_2.

B_1				B_1OH				B_2			
Bond lengths		**Bond angles**		**Bond lengths**		**Bond angles**		**Bond lengths**		**Bond angles**	
(Å)		**(deg)**		**(Å)**		**(deg)**		**(Å)**		**(deg)**	
R(1,2)	1.475	A(2,1,5)	104.2	R(2,3)	0.9647	A(1,5,6)	117.2	R(7,8)	0.959	A(2,1,3)	107.9
R(1,2)	1.466	A(3,1,5)	108.5	R(2,4)	1.938	A(1,7,8)	115.3	R(7,9)	1.756	A(1,5,6)	162.7
R(1,4)	1.466	A(4,1,5)	108.5	R(2,1)	1.704	A(1,9,10)	118.1	R(9,10)	1.497	A(5,6,7)	105.0
R(1,5)	1.712	A(8,7,5)	90.5	R(4,11)	1.728	A(5,1,2)	112.3	R(9,11)	1.468	A(5,6,15)	114.7
R(5,6)	0.961	A(9,7,5)	102.2	R(4,13)	1.723	A(7,1,2)	104.5	R(9,12)	1.471	A(5,6,13)	117.8
R(5,7)	1.999	A(10,7,5)	102.2	R(4,15)	1.764	A(1,2,3)	117.05	R(7,6)	1.893	A(6,15,16)	121.9
R(7,8)	1.603	A(1,5,6)	117.3	R(11,12)	0.955	A(4,2,3)	109.5	R(6,13)	1.785	A(6,13,14)	123.5
R(4,9)	1.591	A(7,5,6)	121.1	R(13,14)	0.956	A(2,4,11)	94.94	R(6,15)	1.714	A(6,7,8)	121.3
R(7,10)	1.591			R(15,16)	0.957	A(2,4,13)	105.1	R(13,14)	0.955	A(7,9,11)	110.9
				R(1,5)	1.633	A(2,4,15)	99.03	R(15,16)	0.957	A(8,7,9)	117.6
				R(1,7)	1.632	A(4,11,12)	121.9	R(5,6)	1.708	A(7,9,10)	109.6
				R(1,9)	1.612	A(4,13,14)	121.3	R(1,5)	1.630	A(7,9,11)	110.9
				R(5,6)	0.958	A(4,15,16)	119.9	R(1,2)	1.482		
				R(7,8)	0.9599			R(1,3)	1.481		
				R(9,10)	0.9908			R(1,4)	1.481		
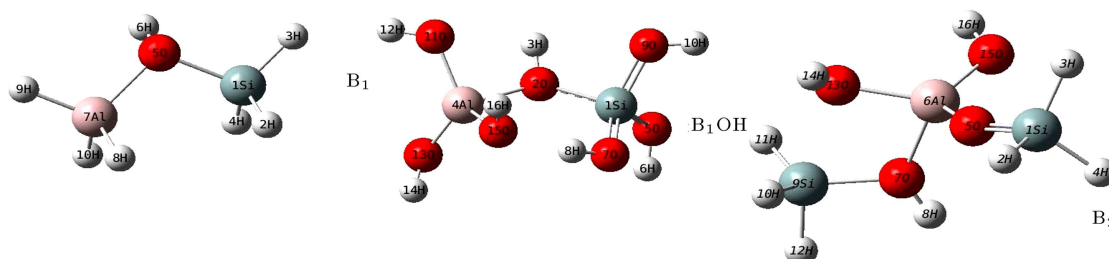
Figure 1. Structures of the B_1, B_1OH, and B_2 clusters.
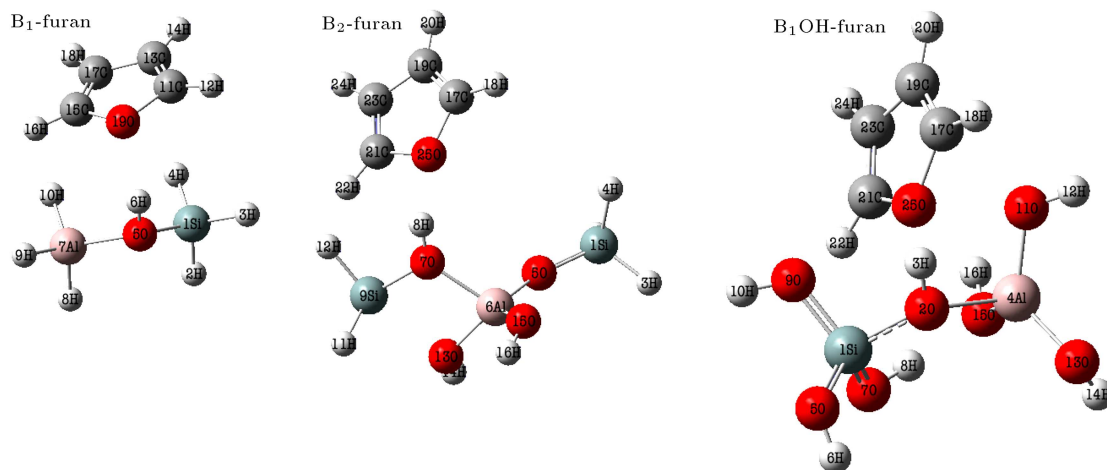
Figure 2. Structures of the B_1-furan, B_1OH-furan, and B_2-furan clusters.

responding geometrical parameters for the B_1−furan, B_1OH−furan, and B_2−furan complexes are reported in Tables 1 and 2.

The total energies ($−E_t$/hartrees), dipole moment (μ/debyes), and Mulliken atomic charges for Al, Si,

O, and H atoms of furan, clusters, and complexes are reported in Table 3. The interaction energy (E_i) is an important theoretical measure for strength of the formation of the studied complexes. It is calculated from the difference between the total energies of

Table 2. Selected ground-state geometry parameters of B_1−furan, B_1OH−furan, and B_2−furan.

B_1−furan				B_1OH−furan				B_2−furan			
Bond lengths (Å)		Bond angles (deg)		Bond lengths (Å)		Bond angles (deg)		Bond lengths (Å)		Bond angles (deg)	
R(1,2)	1.474	A(3,1,4)	110.31	R(1,2)	1.739	A(1,2,3)	116.4	R(1,2)	1.488	A(2,1,3)	107.9
R(1,3)	1.484	A(2,1,5)	106.9	R(3,2)	0.989	A(1,2,4)	117.3	R(1,3)	1.488	A(3,1,4)	107.9
R(1,5)	1.715	A(1,5,6)	117.7	R(2,4)	1.909	A(5,1,2)	103.3	R(1,4)	1.489	A(2,1,5)	110.6
R(5,6)	0.986	A(1,5,7)	123.9	R(1,5)	1.632	A(5,1,7)	119.1	R(1,5)	1.622	A(4,1,5)	110.7
R(5,7)	2.005	A(6,5,7)	114.9	R(1,7)	1.628	A(1,5,6)	112.2	R(5,6)	1.711	A(3,1,5)	111.9
R(7,8)	1.606	A(5,7,8)	95.92	R(1,9)	1.641	A(1,7,8)	113.6	R(6,7)	1.921	A(1,5,6)	166.0
R(7,9)	1.598	A(5,7,10)	98.84	R(5,6)	0.987	A(7,1,9)	108.6	R(6,13)	1.736	A(5,6,13)	118.3
R(7,10)	1.608	A(5,6,19)	173.4	R(4,11)	1.737	A(2,4,11)	105.9	R(6,15)	1.734	A(5,6,15)	114.4
R(6,19)	1.796	A(6,19,14)	120.9	R(4,13)	1.761	A(2,4,13)	95.51	R(13,14)	0.955	A(6,13,14)	123.1
R(19,15)	1.376	A(6,19,15)	131.7	R(4,15)	1.758	A(4,13,14)	118.9	R(15,16)	0.956	A(6,15,16)	119.7
R(19,14)	1.378	A(19,14,18)	115.2	R(10,16)	1.620	A(4,15,16)	121.5	R(7,8)	0.980	A(5,6,7)	105.8
R(14,13)	1.358	A(19,15,16)	115.8	R(10,18)	1.633	A(2,3,25)	173.3	R(17,9)	1.718	A(6,7,8)	117.5
R(13,11)	1.439	A(13,14,19)	109.6	R(14,15)	0.978	A(3,25,20)	122.1	R(9,11)	1.472	A(8,7,9)	117.9
R(15,11)	1.358	A(11,15,19)	109.7	R(11,12)	0.977	A(3,25,21)	130.2	R(9,10)	1.470	A(6,7,9)	121.8
R(11,12)	1.081	A(17,13,11)	127.1	R(15,16)	0.965	A(20,25,21)	107.5	R(9,12)	1.484	A(7,8,10)	108.7
R(17,13)	1.081	A(12,11,15)	126.2	R(13,14)	0.966	A(25,20,24)	114.7	R(8,25)	1.761	A(7,9,11)	111.1
R(14,18)	1.080			R(3,25)	1.754			R(25,21)	1.376	A(7,8,25)	170.8
R(16,15)	1.079			R(20,25)	1.378			R(21,22)	1.078	A(21,25,8)	119.0
				R(25,21)	1.375			R(21,17)	1.350	A(8,25,20)	133.6
				R(20,24)	1.081			R(17,18)	1.076	A(22,21,25)	114.9
				R(21,22)	1.079			R(17,19)	1.434	A(24,20,25)	116.1
								R(19,23)	1.076		
								R(19,20)	1.350		
								R(20,24)	1.074		

Table 3. Total energies ($-E_t$/hartrees), interaction energies (E_i/hartree), and Mulliken atomic charges of $q(Al)$, $q(Si)$, $q(Si')$, $q(O)$, $q(H)$, and $q(O_{furan})$ atoms of furan, cluster, and complexes.

	$-E_t$	E_i	μ	$q(Al)$	$q(Si)$	$q(Si')$	$q(O)^a$	$(H)^a$	$q(O_{furan})$
Furan	230.1		0.7340						-0.410
B_1	611.5		4.700	1.050	1.197		-1.087	0.527	
B_1OH	1063.4		1.660	2.020	2.397		-2.226	0.539	
B_2	1128.2		4.031	2.066	1.207	1.274	-1.093	0.528	
B_1−Furan	841.6	-0.0118	5.647	1.054	1.202		-1.106	0.5442	-0.4713
B_1OH−Furan	1293.5	-0.0161	3.526	2.019	2.402		-1.139	0.5439	-0.4709
B_2−Furan	1376.7	-0.0141	4.166	2.064	1.276	1.208	-1.182	0.478	-0.475

^{a} : O and H atoms are atoms of the OH bridge group of zelite.

zeolite−furan (E_z−furan) complex and isolated species (E_z+E_{furan}) at MP2/cc-PVTZ level of theory and is reported in Table 3. The values of the E_i quantity are negative, indicating that the furan—zeolite interaction is attractive. The charge distribution taken in terms of the Mulliken populations is displayed in Table 3. From these, it seems that there exists a significant variation into the O atom populations of the furan moiety. Furan behaves as an electron acceptor so that negative charge of the O atom increases and electronic charge migration occurs from the zeolite structure to the O atom of furan.

3.2. Vibrational properties
The harmonic vibrational OH frequency of zeolite clusters and the corresponding furan complexes were

vibrational frequencies of the bridged OH stretching mode (cm^{-1}) of B$_1$, B$_1$–furan, B$_1$OH, B$_1$OH–Furan, B$_2$, and B$_2$–furan are 3849.06, 3490.74, 3803.89, 3450.34, 3855.96, and 3461.42 cm^{-1}, respectively. The experimental vibrational frequency of the bridged OH of B$_2$ is 3610 cm^{-1} [19].
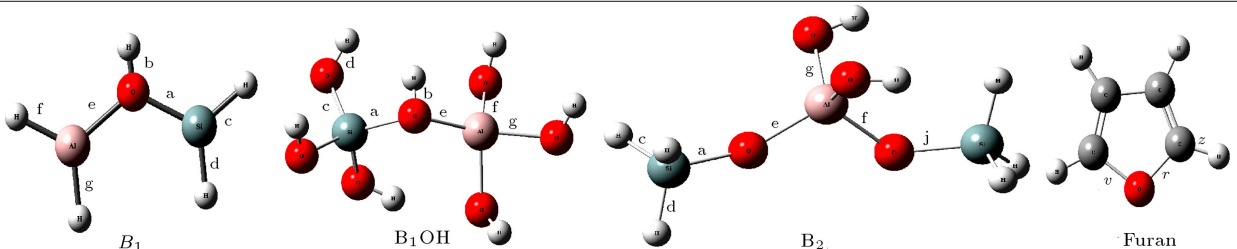
The difference between vibrational frequencies of the bridged OH groups in zeolites and their corresponding complexes is named frequency shift, Δv. Δv for B$_1$, B$_1$OH, and B$_2$ are 358.32, 353.55, and 394.54 cm^{-1}, respectively. The obtained results show that OH stretching vibrational frequency in isolated zeolites is more than the one in furan complexes. So the interaction of furan with OH groups produces a contraction in the OH frequency.
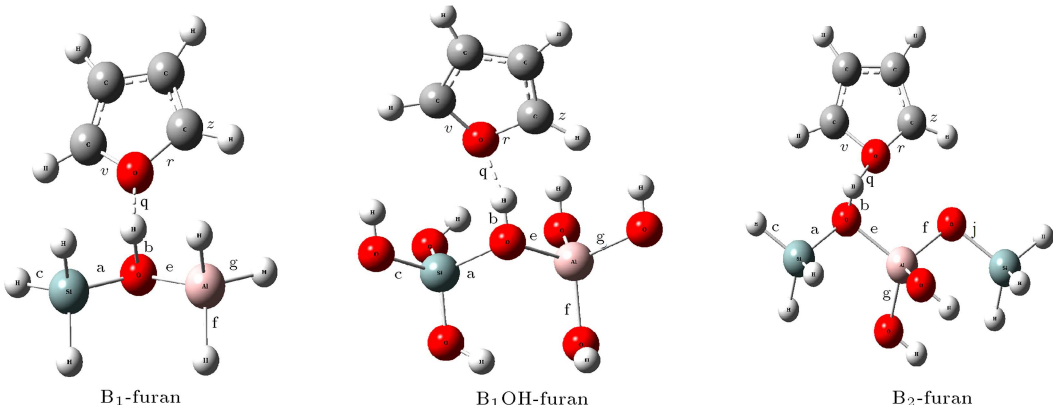
3.3. Topologic properties

The topologic properties for the zeolite clusters and complexes, $\rho(r)$, $\nabla^2\rho(r)$, and ellipticity (ε), are evaluated at the position of CP in the bond paths of all the molecular structures. The topologic properties of charge distribution of the furan molecule and the B$_1$, B$_1$OH, and B$_2$ zeolite clusters are reported in Table 4. All of these data are given for the B$_1$–furan, B$_1$OH–furan, and B$_2$–furan complexes in Table 5. In particular, the absolute value, $\nabla^2\rho(r)$, of the Si-O bond in B$_1$ is more than that of B$_2$ and B$_1$OH, the absolute value, $\nabla^2\rho(r)$, of the Al–O bonds in B$_1$OH is more than that of the other clusters. These results show how

the nature of the chemical environment determines the nature of the dominant interaction in Al–O and Si–O of zeolites. Sensitivity of these bonds in the B$_1$–furan complex are more than in other complexes. The Si–O and Al–O bonds are dominated by ionic interaction as suggested by the negative values of $\nabla^2\rho(r)$. Analysis of the results shows that for the B$_1$OH–furan and B$_2$–furan complexes the interaction does not affect significantly the main topologic properties of the Si–O, Al–O, and O–H bonds. Topologic properties and CP of the O$_{furan}$–(HO)$_{zeolite}$ bonds are shown in Table 5. The values of $\rho(r)$ and $\nabla^2\rho(r)$ at the O–H$_{zeolite}$ CP are relatively lower than those corresponding to the normal bond paths of the other bonds in the studied molecules. Furthermore, the value of $\nabla^2\rho(r)$ at the CP of this bond is also low; these values are negative, so the dominant interaction in this O–H bond is weakly polar. The values of $\nabla^2\rho(r)$ corresponding to the critical points of this weak bond are -0.0234, -0.0240, and -0.0236 a.u for the B$_1$–furan, B$_1$OH–furan, and B$_2$–furan complexes, respectively. However, by formation of the furan-zeolite complex, a weak bond is formed between the O atom of the furan and the H bond of the OH group of zeolite. Ellipticity is the other important topological property of $\rho(r)$ which shows the charge is preferentially accumulated within a bond in a molecule. However, the value of ε at the CP position of the O–(HO)$_{zeolite}$ bond of interaction reveals that a significant accumulation of charge occurs in this

Table 4. Topological properties of the charge density at the bond critical point of furan, B$_1$, B$_1$OH, and B$_2$, total density $\rho(r)$, Laplacian density $\nabla^2\rho(r)$, and ellipticity ε.

	Molecule	a	b	c	e	f	g	j	q	r	v	z
$\rho(r)$	Furan									0.2874	0.3461	0.3015
	B$_1$	0.0044	0.3640	0.1275	0.1239	0.1165	0.0773	0.0793				
	B$_1$OH	0.1187	0.3589	0.1454	0.1451	0.0535	0.1013	0.1032				
	B$_2$	0.1129	0.3642	0.1282	0.1227	0.0532	0.1002	0.3707	0.1417			
$\nabla^2\rho(r)$	Furan									0.2603	0.2722	0.3018
	B$_1$	-0.0703	0.6748	-0.0460	-0.4636	-0.1661	-0.0600	-0.0614				
	B$_1$OH	-0.1639	0.6715	-0.2279	-0.2277	-0.0891	-0.1933	-0.1972				
	B$_2$	-0.1521	0.6779	-0.0471	-0.0461	-0.0918	-0.2008	0.6619	-0.2389			
ε	Furan									0.1300	0.2064	0.2973
	B$_1$	0.0023	0.0088	0.0367	0.0309	0.0799	0.0007	0.0103				
	B$_1$OH	0.0748	0.0092	0.0938	0.0894	0.0362	0.0779	0.0836				
	B$_2$	0.0722	0.0096	0.0289	0.0310	0.0178	0.0190	0.0015	0.0017			

Table 5. Topological properties of the charge density at the critical point of B_1−furan, B_1OH−furan, and B_2−furan complexes.

B₁-furan   B₁OH-furan   B₂-furan

	Molecule	a	b	c	e	f	g	j	q	r	v	z
	B₁-furan	0.1204	0.3415	0.1235	0.0479	0.0771	0.0776		0.0368	0.2751	0.2774	0.3031
$\rho(r)$	**B₁OH-furan**	0.1146	0.3384	0.1006	0.0611	0.1006	0.0956	0.3703	0.0393	0.2778	0.2751	0.3023
	B₂-furan	0.1173	0.3398		0.0569	0.0996	0.0980	0.1423	0.0379	0.0569	0.2776	0.3027
	B₁-furan	-0.1735	0.6364	-0.0458	-0.0768	-0.0596	-0.0583		-0.0234	0.0566	0.0594	0.3165
$\nabla^2\rho(r)$	**B₁OH-furan**	-0.1589	0.6298	-0.1895	-0.1040	-0.1895	-0.1789	0.0824	-0.0239	0.0603	0.0555	0.3133
	B₂-furan	-0.1670	0.6353		-0.0962	-0.2002	-0.1863	-0.2401	-0.0236	-0.0922	0.0752	0.3174
	B₁-furan	0.0731	0.0069	0.0341	0.0190	0.0115	0.0067		0.0486	0.0943	0.1263	0.0503
ε	**B₁OH-furan**	0.0631	0.0133	0.0491	0.0912	0.0535	0.0816	0.0761	0.0480	0.1212	0.0848	0.0539
	B₂-furan	0.0732	0.0073		0.0241	0.0156	0.0731	0.0031	0.1131	0.2405	0.2386	0.0287

bond. The values of ε for B_1−furan, B_1OH−furan, and B_2−furan complexes are 0.0486, 0.0480, and 0.1131, respectively.

3.4. Global reactivity descriptors

A large part of the theoretical chemistry related to reactivity is based on the concept of the Frontier Molecular Orbitals (FMO), especially the Lowest Unoccupied Molecular Orbital (LUMO) and the Highest Occupied Molecular Orbital (HOMO). Interaction between these orbitals often allows for a good description of the reactivity of reactions. The FMO theory says that attack of an electrophilic species will take place where there is more density of the HOMO, whereas attack of a nucleophilic species will take place in a region with higher density of the LUMO. Parr and coworkers have demonstrated that nearly the whole frontier molecular theory can be rationalized from the Density Functional Theory (DFT) [20].

Chemical potential (μ) and molecular hardness (η) for the N-electron system with the total energy of E and external potential of $V(r)$ are defined respectively as the first and second derivatives of energy with respect to N [21,22]:

$$\mu = \left[\frac{\partial E}{\partial N}\right]_{V(\vec{r})} = -\chi, \tag{1}$$

and:

$$\eta = \frac{1}{2}\left[\frac{\partial^2 E}{\partial N^2}\right]_{V(\vec{r})} = \frac{1}{2}\left[\frac{\partial \mu}{\partial N}\right], \tag{2}$$

where $\chi(eV)$ in Eq. (1) is electronegativity. In numerical applications, μ and η are calculated through the use of difference approximation:

$$\mu = -\frac{1}{2}\left(\text{IP} + E_A\right), \tag{3}$$

$$\eta = \frac{1}{2}\left(\text{IP} - E_A\right). \tag{4}$$

Vertical Ionization Potential (IP) and Electron Affinity (E_A) can be obtained from the energy of neutral, anionic, and cationic species at the geometry of corresponding N electron neutral species, as follows:

$$\text{IP} = \left[E(N-1) - E(N)\right]. \tag{5}$$

$$E_A = \left[E(N) - E(N+1)\right], \tag{6}$$

Eqs. (3) and (4) can be simplified by using Koopmans' theorem Parr and Yang [13] which approximates electronic affinity and ionization potential to the negative of LUMO energy (E_{LUMO}) and HOMO energy (E_{HOMO}), respectively.

$$\mu = -\frac{1}{2}\left(E_{\text{LUMO}} + E_{\text{HOMO}}\right), \qquad (7)$$

$$\eta = \frac{1}{2}\left(E_{\text{LUMO}} - E_{\text{HOMO}}\right). \qquad (8)$$

Electrophilicity index (ω) and global softness (S) are defined as follows:

$$\omega = \frac{\mu^2}{2\eta}, \qquad (9)$$

$$S = 1/\eta. \qquad (10)$$

According to Parr et al. [22], electrophilicity index (ω) is a global reactivity index similar to chemical hardness and chemical potential. This new reactivity index measures the stabilization in energy when the system reserves additional electronic charge (ΔN). The direction of charge transfer is determined by the electronic chemical potential of molecule because an electrophile is a chemical species capable of accepting electrons from the environment; its energy must decrease upon accepting electronic charge. So its electronic chemical potential must be negative. The E_{HOMO} and E_{LUMO} band gap, χ, μ, η, S, and ω for furan and zeolites molecules are listed in Table 6.

In a reaction between two molecules, species can act as a nucleophile which has a lower value of electrophilicity index. The values of electrophilicity index listed in Table 6 show that B_1, B_1OH, and B_2 are good nucleophiles so that they can attack the furan. Electrophilic Charge Transfer (ECT) [23] is explained as the difference between $\Delta N_{\max}$ values of interacting molecules. We consider two molecules A (furan) and B (B_1, B_1OH, and B_2) approach each other, where two cases exit: (i) ECT > 0, charge flow from B to A; and (ii) ECT < 0, charge flow from A to B. ECT is calculated by the following equation:

$$\text{ECT} = \left(\Delta N_{\max}\right)_A - \left(\Delta N_{\max}\right)_B, \qquad (11)$$

where $(\Delta N_{\max})_A = \mu_A/\eta_A$ and $(\Delta N_{\max})_B = \mu_B/\eta_B$.

ECT is calculated as 0.306, 0.255, and 0.271 for the B_1−furan, B_1OH−furan, and B_2−furan complexes, respectively. These results show that electrons are transferred from the zeolites to the furan. Therefore, the furan treats as electron acceptor and so all the zeolites treat as electron donor. So furan has electrophilic

behavior because the value of chemical potential is low and also the value of electrophilicity index is high. As shown in Table 6, the high value of chemical potential and the low value of electrophilicity index for these zeolites favor the nucleophilic behavior of furan.

3.5. Local reactivity descriptors

The Fukui Function (FF) [24,25] or frontier function (f_k^+, f_k^-) measures changes in number of the electrons (removing electrons from the HOMO or adding electrons to the LUMO, respectively) in chemical reactions and has been used to predict the reactivity of sites in a molecule. This function is a local density functional descriptor which is calculated using the procedure proposed based on a finite difference method [25].

In this work, the two functions f^+ and f^- were used to determine electrophilic and nucleophilic attacks, respectively. These functions can be given by:

$$f_k^+ = q_k^{(N+1)} - q_k^{(N)} \quad \text{for atom k as an electrophile}$$

$$f_k^- = q_k^{(N)} - q_k^{(N-1)} \quad \text{for atom k as an nucleophile}$$

where the parameters $q_k^{(N)}$, $q_k^{(N-1)}$, and $q_k^{(N+1)}$ are the charges of atom k calculated in the N, $N-1$, and $N+1$ electron systems, respectively, at the optimized geometry of the molecule with N electrons. In the past few years, the condensed Fukui functions have been used to explain the regioselectivity in chemical reactions [26]. It is a tool that allows prediction of which electron or moiety of a molecule will display more or less nucleophilic or electrophilic characters. These functions are calculated at MP2/cc-PVTZ level of theory. The electrophilic reactivity descriptors (f_k^+) and nucleophilic reactivity descriptors (f_k^-) for all molecules are listed in Table 7. Maximum values of the nucleophilic reactivity descriptors at H_6, H_{14}, and H_8 indicate that these sites are more prone to electrophilic attack in B_1, B_1OH, and B_2 molecules, respectively. So we can say that the H atom of the bridged OH group of zeolite clusters attack the O atom of furan in zeolite complexes.

4. Conclusions

The structural, vibrational, and topologic properties of the molecular complexes between furan and a series

Table 6. Calculated $\varepsilon_{\text{HOMU}}$, $\varepsilon_{\text{LUMO}}$, χ, μ, η, S, and ω for furan, B_1OH B_2, and B_1.

Sample	$\varepsilon_{\text{HOMU}}$ (eV)	$\varepsilon_{\text{LUMO}}$ (eV)	χ (eV)	μ (eV)	η (eV)	S (eV)	ω (eV)
Furan	-0.3165	0.14871	0.0839	-0.0839	0.2326	0.1164	0.1510
B_1OH	-0.4637	0.1102	0.1768	-0.1768	0.2869	0.1435	0.0544
B_2	-0.4355	0.0981	0.1687	-0.1687	0.2668	0.1334	0.0533
B_1	-0.3910	0.0780	0.1565	-0.1565	0.2345	0.1173	0.0522

Table 7. Selected reactivity descriptors indexes of the furan, B_1, B_2, and B_1OH compounds.

		$q(N)$	$q(N-1)$	$q(N+1)$	f_k^+	f_k^-
Furan	**O**	-0.4105	-0.1724	-0.3362	0.7467	-0.2381
B_1	**H_6**	0.5276	0.5466	0.4160	-0.1116	-0.019
B_2	**H_8**	0.5310	0.5464	0.3888	-0.1422	-0.0154
	H_{14}	0.4963	0.5136	0.4426	-0.0537	-0.0173
	H_{16}	0.4792	0.5019	0.4472	-0.0320	-0.0227
B_1OH	**H_3**	0.5499	0.5652	0.4401	-0.1098	-0.0153
	H_6	0.5068	0.5217	0.4068	-0.01	-0.0149
	H_8	0.5322	0.5309	0.4981	-0.0341	0.0013
	H_{10}	0.5059	0.5316	0.3807	-0.1252	-0.0257
	H_{12}	0.4831	0.5155	0.4244	-0.0587	-0.0324
	H_{14}	0.4820	0.5163	0.4361	-0.0459	-0.0343
	H_{16}	0.4906	0.5217	0.4298	-0.0608	-0.0311

of B_1, B_1OH, and B_2 clusters have been studied at MP2/cc-PVTZ level of theory. The Laplacian of electron density at the critical points in the bonds path of the furan-zeolite complex shows that a weak bond is formed between the O atom of furan and the H bond of the OH group of zeolite. The hydrogen bonding between the O atom of the furan molecule and the OH zeolite groups has been assigned as the dominant interaction. We have shown that OH frequencies of the bridged groups are decreased by the effect of complex formation in the adsorption of furan into zeolites. Electrophilic Charge Transfer (ECT) confirms that electrons are transferred from the zeolites to the furan. So the furan treats as the electron acceptor and all the zeolites treat as the electron donor. The results of Fukui functions represent the zeolites active sites for attack to the O atom of furan.

References

1. Lee, H.-K., Chan, K.-F., Hui, C.-W., Yim, H.-K., Wu, X.-W. and Wong, H.N. "Use of furans in synthesis of bioactive compounds", *Pure. Appl. Chem.*, **77**(1), pp. 139-143 (2005).

2. Ratajczak, H. and Orville-Thomas, W.J., *Molecular Interactions*, Eds., **2**, Wiley, Chichester, UK, pp. 1-100 (1981).

3. Gur'yanova, E.N., Gol'dshtein, I.P. and Perepelkova, T.I. "The polarity and strength of the intermolecular hydrogen bond", *Russ. Chem. Rev.*, **45**, pp. 792-806 (1976).

4. Corma, A. "Solid acid catalysts", *Chem, Rev.*, **97**, pp. 2373-2420 (1997).

5. Vansant, E.F. "Molecular engineering of oxides and zeolites", *J. Mol. Catal. A Chem.*, **115**, pp. 379-387 (1997).

6. Holm, M., Taarning, E., Egeblad, K. and Christensen, C.H. "Catalysis with hierarchical zeolites", *Catal. Today.*, **168**(1), pp. 3-16 (2011).

7. Hinchliffe, A. and Soscún, H. "Ab initio studies of the dipole polarizabilities of conjugated molecules. Part 5. The five-membered heterocyclics C_4H_4E (E = BH, AlH, CH_2, SiH_2, NH, PH, 0 and S)", *J. Mol. Struct. Theochem.*, **331**, pp. 109-125 (1995).

8. Soscún, H., Castellano, O., Hernández, J. and Hinchliffe, A. "Theoretical study of the structural, vibrational, and topologic, properties of the charge distribution of the molecular complexes between thiophene and Brönsted acid sites of zeolites", *Int. J. Quantum. Chem.*, **87**, pp. 240-253 (2002).

9. Zecchina, A., Geobaldo, F., Spoto, G., Bordiga, S., Ricchiardi, G., Buzzoni R. and Petrini, G. "FTIR investigation of the formation of neutral and ionic hydrogen-bonded complexes by interaction of H-ZSM-5 and H-mordenite with CH_3CN and H_2O: Comparison with the H-NAFION superacidic system", *J. Phys. Chem.*, **100**(41), pp. 16584-16599 (1996).

10. Zecchina, A., Bordiga, S., Spoto, G., Scarano, D., Spanò, G. and Geobaldo, F. "IR spectroscopy of neutral and ionic hydrogen-bonded complexes formed upon interaction of CH_3OH, C_2H_5OH, $(CH_3)_2O$, $(C_2H_5)_2O$ and C_4H_8O with H-Y, H-ZSM-5 and H-mordenite: Comparison with analogous adducts formed on the H-Nafion superacidic membrane", *J. Chem. Soc., Faraday Trans.*, **92**, pp. 4863-4875 (1996).

11. Spoto, G., Geobaldo, F., Bordiga, S., Lamberti, C., Scarano, D. and Zecchina, A. "Heterocycles oligomerization in acidic zeolites: A UV-visible and IR study", *Top. Catal.*, **8**(3), pp. 279-292 (1999).

12. Hehre, W.J., Radom, L., Schleyer, P.V.R. and Pople, J., *Ab Initio Molecular Orbital Theory*, Wiley Interscience, New York (1986).

13. Parr, R.G. and Yang, W., *Density Functional Theory of Atoms and Molecules*, Oxford University Press, New York (1989).

14. Bader, R.F. and MacDougall, P.J. "Toward a theory of chemical reactivity based on the charge density", *J. Am. Chem. Soc.*, **107**(24), pp. 6788-6795 (1985).

15. Cioslowski, J. and Stefanov, B.B. "Variational determination of the zero-flux surfaces of atoms in molecules", *Mol. Phys.*, **84**(4), pp. 707-716 (1995).

16. Frisch, M.J., Trucks, G.W., Schlegel, H.B., Gill, P.M.W., Johnson, B.G., Robb, M.A., Cheeseman, J.R., Keith, T.A., Peterson, G.A., Montgomery, J.A., Raghavachari, K., AlLaham, M.A., Zakrzewski, V.G., Ortiz, J.V., Foresman, J.B., Cioslowski, J., Stafanov, B.B., Nanayakkara, A., Challacombe, M., Peng, C.Y., Ayala, P.Y., Chen, W., Wong, M.W., Andres, J.L., Replogle, E.S., Gomperts, R., Martin, R.L., Fox, D.J., Binkley, J.S., Defrees, D.J., Baker, J., Stewart, J.P., Head Gordon, M., Gonzalez, C. and Pople, J.A., *Gaus-*

sian 03 Revision B.04, Gaussian, Inc., Wallingford CT (2004).

17. Mellouki, A., Liévin, J. and Herman, M. "The vibrational spectrum of pyrrole (C_4H_5N) and furan (C_4H_4O) in the gas phase", *Chem. Phys.*, **271**, pp. 239-266 (2001).

18. Szafran, M. and Koput, J. "Ab initio and DFT calculations of structure and vibrational spectra of pyridine and its isotopomers", *J. Mol. Struct.*, **565**, pp. 439-448 (2002).

19. Garcia, C.L. and Lercher, J.A. "Adsorption and surface reactions of thiophene on ZSM 5 zeolites", *J. Phys. Chem.*, **96**(6), pp. 2669-2675 (1992).

20. Parr, R.G. and Pearson, R.G. "Absolute hardness: Companion parameter to absolute electronegativity", *J. Am. Chem. Soc.*, **105**(26), pp. 7512-7516 (1983).

21. Geerlings, P., De Proft, F. and Langenaeker, W. "Conceptual density functional theory", *Chem. Rev.*, **103**(5), pp. 1793-1874 (2003).

22. Parr, R.G., Szentpály, L. and Liu, S. "Electrophilicity index", *J. Am. Chem. Soc.*, **121**(9), pp. 1922-1924 (1999).

23. Padmanabhan, J., Parthasarathi, R., Subramaniaan, V. and Chattaraj, P.K. "Electrophilicity-based charge transfer descriptor", *J. Phys. Chem. A.*, **111**(7), pp. 1358-1368 (2007).

24. Senthilkumar, K., Ramaswamy, M. and Kolandaivel, P. "Studies of chemical hardness and Fukui function using the exact solution of the density functional theory", *Int. J. Quantum. Chem.*, **81**, pp. 4-10 (2001).

25. Parr, R.G. and Yang, W. "Density functional approach to the frontier-electron theory of chemical reactivity", *J. Am. Chem. Soc.*, **106**(14), pp. 4049-4050 (1984).

26. Yang, W. and Mortier, W.J. "The use of global and local molecular parameters for the analysis of the gas-phase basicity of amines", *J. Am. Chem. Soc.*, **108**(19), pp. 5708-5711 (1986).

Biographies

Leila Zeidabadinejad was born in Kerman, Iran, in 1987. She received her BS degree in Chemistry from Shahid Bahonar University, Kerman, Iran, in 2008, and her MS degree in Physical Chemistry from Sharif University of Technology (Iran) in 2011. She is currently working on her PhD in Physical Chemistry under the supervision of Professor Maryam Dehestani at the Physical Chemistry Department in Shahid Bahonar University of Kerman, Iran. Her main research interests include quantum chemistry and molecular spectroscopy in Physical Chemistry.

Maryam Dehestani was born in Kerman, Iran, in 1967. She received a BS degree in Chemistry from Shahid Bahonar University, Kerman, Iran, in 1988, and MS and PhD degrees in Physical Chemistry from Tarbiat-Moalem University, Iran, in 1991 and 2001, respectively. She has been a faculty member at the Department of Chemistry in Shahid Bahonar University of Kerman, Iran, since 2002. Her research interests include quantum chemistry, molecular spectroscopy, computational chemistry, and nanostructures calculations. She is the author and co-author of about 90 papers in cited journals and conferences.